Engineering Conferences International
ECI Digital Archives

5th International Conference on Porous Media and Their Applications in Science, Engineering and Industry

Refereed Proceedings

Summer 6-24-2014

Numerical Simulation of 3-D free convection in porous media due to combined surface forced convection and internal heat generation

Kevin Anderson
California State Polytechnic University - Pomona

Maryann Shafahi
California State Polytechnic University - Pomona

Shawn McGann
California State Polytechnic University - Pomona

Watit Pakdee
Thamasat University

Proceedings of the 5th International Conference on Porous Media and its Applications in Science and Engineering
ICPM5
June 22-27, 2014, Kona, Hawaii

NUMERICAL SIMULATION OF 3-D FREE CONVECTION IN POROUS MEDIA DUE TO COMBINED SURFACE FORCED CONVECTION AND INTERNAL HEAT GENERATION

Kevin R. Anderson, Maryam Shafahi and Shawn McGann
California State Polytechnic University, Pomona, 91768, USA

Watit Pakdee
Thamasat University, Bangkok, Thailand

ABSTRACT
A three-dimensional fluid-saturated porous medium model for natural convective flow has been developed, taking into account inertial and viscous forces within the fluid. The model consists of a cube with a top surface partially exposed to a steady, uniform convective heat flux and the entire domain to uniform internal heat generation. The differential equations for the Brinkman-extended Darcy model were formulated and non-dimensionalized, with numerical solutions obtained using the Galerkin finite element method. The results have been validated by comparison with previously published reports. It has been observed that the applied boundary conditions result in a central toroidal vortex driven by buoyancy, which in turn influences the isothermal profile. The shape and intensity of these vortices is significantly affected by a combination of dimensionless parameters such as Rayleigh number, Darcy number, and porosity.

INTRODUCTION
Natural convection in porous media by surface convection and internal heat generation exist in a variety of engineering applications, such as geothermal reservoirs, underground water flow, and solar collectors [1]. The chemical and nuclear industries also have applications, with internal heat generation arising through radioactive decay or exothermic reactions [2,3]. Compost piles have also exhibited similar characteristics, with internal heat generation resulting from micro-organisms undergoing exothermic reactions to break down waste [4].

Flow in a porous medium has been studied extensively using a variety of experimental and numerical methods for both internal heat generation [5-10] and surface convection [11-14]. Vishnampet et al. [15] examined natural convection in a two-dimensional porous enclosure using the lattice Boltzmann method. The study consisted of an insulated square enclosure with one side heated to a uniform temperature and the other wall cooled. High porous Rayleigh numbers were examined in order to determine form drag due to the porous media.

Kramer et al. [16] published a study of three-dimensional flow in porous media using the boundary element method to examine the effects of the Rayleigh and Darcy numbers on temperature and velocity profiles. A hot and cold wall was used to generate natural convection using the Brinkman-extended Darcy model coupled with the energy equation using Boussinesq approximation.

Pakdee and Rattanadecho [17] performed analysis on transient natural convection through porous media in a rectangular cavity with a convective surface boundary condition. The geometry consisted of an insulated square cavity with a portion of the top subjected to convective ambient air. The focus was the resulting temperature contours and streamlines for various Rayleigh numbers, Darcy numbers, and convection coefficients. The study concluded that the convective boundary condition resulted in two symmetrical eddies initiated from the buoyancy effect, triggered by a lateral temperature gradient near the top surface. Smaller values of the Darcy number impeded these eddies and larger Rayleigh numbers increased streamline intensities, allowing the flow to penetrate further downward.

In this study, the work of Pakdee and Rattandecho [7] is extended to include three-dimensional effects inside an insulated cube exposed to partial top layer convection and internal heat generation. The parametric study examines the influence of various Rayleigh numbers, Darcy numbers, and porosity on the flow field and isothermal profiles within an isotropic fluid-saturated porous medium. The Brinkman-extended Darcy model is applied, assuming constant thermal properties and accounting for buoyancy forces using the Boussinesq

approximation. The differential formulation is discretized

NOMENCLATURE

C	=	Specific heat (J/kg-K)
Da	=	Darcy number
g	=	Gravitational constant
H	=	Cavity height/width/depth
h	=	Convective heat transfer coefficient
k	=	Effective thermal conductivity
P	=	Pressure
Pr	=	Prandtl number
Ra	=	Rayleigh number
T	=	Temperature
t	=	Time
u,v,w	=	Velocity components
X,Y,Z	=	Dimensionless Cartesian coordinates

Greek Symbols

α	=	Thermal diffusivity
κ	=	Permeability
ε	=	Porosity
μ	=	Dynamic viscosity
ν	=	Kinematic viscosity
ρ	=	Density
τ	=	Dimensionless time
θ	=	Dimensionless temperature
ω	=	Vorticity
ζ	=	Dimensionless vorticity
ψ	=	Stream function
Ψ	=	Dimensionless stream function

Subscripts

f	=	Fluid
o	=	Initial condition
∞	=	Ambient condition

PROBLEM DESCRIPTION

The computational domain is a three-dimensional cube enclosure filled with fluid-saturated porous medium as shown in Figure 1. All domain boundaries are adiabatic except for an exposed square portion at the top of the enclosure, which is subject to a convective boundary condition. Additionally, there is a constant, uniform, isotropic internal heat source across the entire domain.

The porous medium is assumed thermally isotropic, homogeneous, and comprised of spherical particles with uniform permeability and porosity within the enclosure. The thermophysical properties of the porous medium are considered constant, with the saturating incompressible fluid in local thermodynamic equilibrium. Buoyancy forces resulting from the variation of density are taken into account by the Boussinesq approximation.

and solved using the Galerkin finite element method. The initial and boundary conditions for the geometry depicted in Figure 1 are given as:

$$u = v = w = 0, \quad T = T_o \quad \text{for} \quad t = 0 \tag{1}$$

$$u = v = w = 0 \quad \text{at} \quad x = y = z = 0 \text{ and } x = y = z = H \tag{2}$$

$$\frac{\partial T}{\partial x} = 0 \quad \text{at } x = 0 \text{ and } x = H \tag{3}$$

$$\frac{\partial T}{\partial y} = 0 \quad \text{at } y = 0 \text{ and } y = H \tag{4}$$

$$\frac{\partial T}{\partial z} = 0 \quad \text{at } z = 0 \text{ and } z = H,\ 0 \le x \le L \quad H\text{-}L \le x \le H \quad 0 \le y \le L \quad H\text{-}L \le y \le D \tag{5}$$

At the top portion of the cube, the exposed wall boundary condition is given as

$$-k\left(\frac{\partial T}{\partial z}\right) = h\left(T - T_\infty\right) \quad \text{at} \quad z = H \quad L \le x \le H\text{-}L \quad L \le y \le H\text{-}L \tag{6}$$

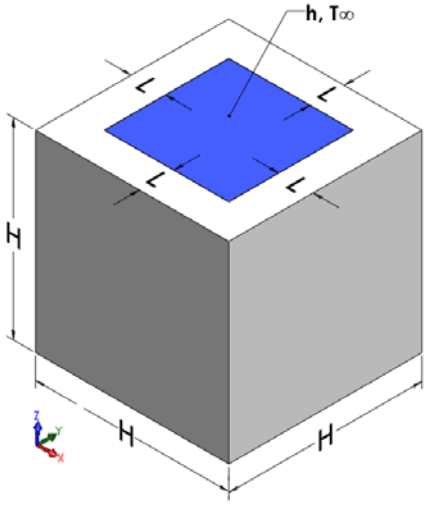

Figure 1. 3D representation of computational domain

and internal heat generation defined by

$$\left(\frac{\partial^2 T}{\partial x^2} + \frac{\partial^2 T}{\partial y^2} + \frac{\partial^2 T}{\partial z^2}\right) + \frac{q'''}{k} = \frac{1}{\alpha}\frac{\partial T}{\partial t} \tag{7}$$

at
$0 \le x \le H$
$0 \le y \le H$
$0 \le z \le H$

where k is the effective thermal conductivity, h is the convective heat transfer coefficient, q''' is internal heat

generation, and α is thermal diffusivity. These boundary conditions are derived from the heat equation.

The governing equations for heat and fluid flow using standard symbols are

Continuity equation

$$\frac{\partial u}{\partial x}+\frac{\partial v}{\partial y}+\frac{\partial w}{\partial z}=0 \tag{8}$$

x-momentum equation

$$\frac{1}{\varepsilon}\frac{\partial u}{\partial t}+\frac{u}{\varepsilon^2}\frac{\partial u}{\partial x}+\frac{v}{\varepsilon^2}\frac{\partial u}{\partial y}+\frac{w}{\varepsilon^2}\frac{\partial u}{\partial z}= -\frac{1}{\rho_f}\frac{\partial P}{\partial x}+\frac{\nu}{\varepsilon}\left(\frac{\partial^2 u}{\partial x^2}+\frac{\partial^2 u}{\partial y^2}+\frac{\partial^2 u}{\partial z^2}\right)-\frac{\mu u}{\rho_f \kappa} \tag{9}$$

y-momentum equation

$$\frac{1}{\varepsilon}\frac{\partial v}{\partial t}+\frac{u}{\varepsilon^2}\frac{\partial v}{\partial x}+\frac{v}{\varepsilon^2}\frac{\partial v}{\partial y}+\frac{w}{\varepsilon^2}\frac{\partial v}{\partial z}= -\frac{1}{\rho_f}\frac{\partial P}{\partial y}+\frac{\nu}{\varepsilon}\left(\frac{\partial^2 v}{\partial x^2}+\frac{\partial^2 v}{\partial y^2}+\frac{\partial^2 v}{\partial z^2}\right)-\frac{\mu v}{\rho_f \kappa} \tag{10}$$

z-momentum equation

$$\frac{1}{\varepsilon}\frac{\partial w}{\partial t}+\frac{u}{\varepsilon^2}\frac{\partial w}{\partial x}+\frac{v}{\varepsilon^2}\frac{\partial w}{\partial y}+\frac{w}{\varepsilon^2}\frac{\partial w}{\partial z}= -\frac{1}{\rho_f}\frac{\partial P}{\partial z}+\frac{\nu}{\varepsilon}\left(\frac{\partial^2 w}{\partial x^2}+\frac{\partial^2 w}{\partial y^2}+\frac{\partial^2 w}{\partial z^2}\right)-\frac{\mu v}{\rho_f \kappa}+g\beta\left(T-T_\infty\right) \tag{11}$$

Energy equation

$$\sigma\frac{\partial T}{\partial t}+u\frac{\partial T}{\partial x}+v\frac{\partial T}{\partial y}+w\frac{\partial T}{\partial z}=\alpha\left(\frac{\partial^2 T}{\partial x^2}+\frac{\partial^2 T}{\partial y^2}+\frac{\partial^2 T}{\partial z^2}\right) \tag{12}$$

where

$$\sigma=\frac{\left[\varepsilon\left(\rho c_p\right)_f+(1-\varepsilon)\left(\rho c_p\right)_s\right]}{\left(\rho c_p\right)_f} \tag{13}$$

and ε is the porosity of the porous medium, ν is the kinematic viscosity, ρ_f is fluid density, κ is the medium permeability, and β is the thermal expansion coefficient. The heat capacity ratio σ of unity is used in the present study. The momentum equations in this form are known as the Brinkman-Extended Darcy model, which accounts for the viscous effects due to the presence of a solid body [19]. Note that when porosity is equal to 1 and removing the Brinkman term along with the Boussinesq approximation, the model reduces to the Navier-Stokes equations.

The variables are non-dimensionalized into the following

$$X=\frac{x}{H},Y=\frac{y}{H},Z=\frac{z}{H},U=\frac{uH}{\alpha}$$
$$V=\frac{vH}{\alpha},\tau=\frac{t\alpha}{H^2},\zeta=\frac{\omega H^2}{\alpha},\Psi=\frac{\psi}{\alpha} \tag{14}$$
$$\theta=\frac{T-T_o}{T_\infty-T_o}$$

and the following dimensionless numbers

$$Ra=\frac{g\beta\left(T_i-T_\infty\right)H^2}{\nu\alpha},Pr=\frac{\nu}{\alpha},Da=\frac{\kappa}{H^2} \tag{15}$$

where α is the effective thermal diffusivity, ν is kinematic viscosity, β is the coefficient of thermal expansion, ζ is the vorticity, ψ is the stream function, and κ is the medium permeability. The Rayleigh number, *Ra* gives the relative magnitude of buoyancy to viscous forces, the Prandtl number, *Pr* is the ratio of fluidic to heat diffusivity, while the Darcy number, *Da* gives the relationship between the medium's permeability and length scale. Permeability is defined as the measure of the ability of a porous material to allow fluid to pass through it, while porosity is fraction of the volume of voids over the total volume.

The governing equations can be written in the standard stream-function / vorticity dimensionless form as follows

$$\frac{\partial^2\Psi}{\partial X^2}+\frac{\partial^2\Psi}{\partial Y^2}+\frac{\partial^2\Psi}{\partial Z^2}=-\zeta \tag{16}$$

$$\varepsilon\frac{\partial\zeta}{\partial\tau}+U\frac{\partial\zeta}{\partial X}+V\frac{\partial\zeta}{\partial Y}+W\frac{\partial\zeta}{\partial Z}= \varepsilon Pr\left(\frac{\partial^2\zeta}{\partial X^2}+\frac{\partial^2\zeta}{\partial Y^2}+\frac{\partial^2\zeta}{\partial Z^2}\right)+\varepsilon^2 Ra\,Pr\left(\frac{\partial\theta}{\partial X}\right)-\frac{\varepsilon^2 Pr}{Da}\zeta \tag{17}$$

$$\sigma\frac{\partial\theta}{\partial\tau}+U\frac{\partial\theta}{\partial X}+V\frac{\partial\theta}{\partial Y}+W\frac{\partial\theta}{\partial Z}= \alpha\left(\frac{\partial^2\theta}{\partial X^2}+\frac{\partial^2\theta}{\partial Y^2}+\frac{\partial^2\theta}{\partial Z^2}\right) \tag{18}$$

NUMERICAL PROCEDURE

Analytical solutions to the partial differential equations (PDE) were obtained using the Galerkin finite element method. Galerkin methods belong to the class of solution methods for PDEs where the solution residue is minimized, giving rise to the well-known weak formulation of problems [20]. However, these nonlinear equations are unstable if discretized using the Galerkin finite element method. In order to obtain numerical

solutions, streamline diffusion is used for these strongly coupled systems of equations [21].

Table 1. Grid independent study

Number of Elements	Maximum Non-dimensional Velocity	Percent Change
16,000	1.665×10^{-3}	-
55,000	1.653×10^{-3}	0.68%
336,000	1.660×10^{-3}	0.38%

A uniform grid resolution of 55,000 tetrahedral elements was found to be sufficient for all computations and time steps. Finer, more computationally expensive grids did not result in significant change as shown in Table 2. Thermal properties of the porous medium were assumed to be constant, with an effective thermal conductivity of 10 W/m-K and a Prandtl number of unity for all studies.

MODEL VALIDATION

The present study was validated by comparing with the results of Nithiarasu et al [18] for natural convection in a rectangular fluid saturated porous cavity. The cavity consists of two opposing isothermal walls and the rest insulated. The original study is performed in two-dimensions, but the validation study is performed in three-dimensions assuming uniform properties and boundary conditions in the added dimension. The results are seen to be in agreement as shown in Table 2.

Table 2. Comparison of results with Nithiarasu [18]

Study	ε	Ra	Da	V_{max}	Difference
Present	0.6	10^4	10^{-2}	9.28	0.64%
Nithiarasu et al [18]				9.34	

RESULTS AND DISCUSSION

All numerical results are taken at non-dimensionalized time sufficient to reach a steady state solution, τ = 0.2475. This agrees with the similar study done by Pakdee and Rattanadecho [17]. The initial non-dimensionalized temperature value for the domain is set to zero, with a constant convective surface boundary condition of 60 W/m^2-K on the partially exposed top surface with an external temperature of 1. A uniform isotropic internal heat source of 1,000 W/m^2 is also applied to all studies. Parametric analysis with the controlling parameters of Darcy number, *Da*, Rayleigh number, *Ra*, and porosity, ε are conducted to assess their influence on streamlines, velocity profiles, and isothermal contours. The coupled boundary conditions are characterized by the formation of a global toroidal vortex, also known as a vortex ring. The vortex formation is a result of buoyancy, induced by thermal gradients disseminated from the partial top surface boundary conditions and amplified by the internal heat generation. The non-uniform thermal gradients at the top of the cube cause the heated portions of the fluid to become lighter and expand laterally. This fluid then contacts the cube's vertical boundaries and flows downward along the four walls. Simultaneously, the internal heat source generates a central thermal concentration, inciting buoyancy forces contributing to the partial surface convection gradient. This fluid motion illustrates that the buoyancy forces are able to overcome the retarding effects of viscous forces.

Figure 3 displays the streamlines and velocity magnitude, illustrating the sensitivity to Darcy number. The larger Darcy number corresponds to higher permeablility, resulting in higher velocity and more convective mixing in the interior. The smaller Darcy number's lower permeability generates a force opposing the flow, which in turn suppresses the the driving thermal currents

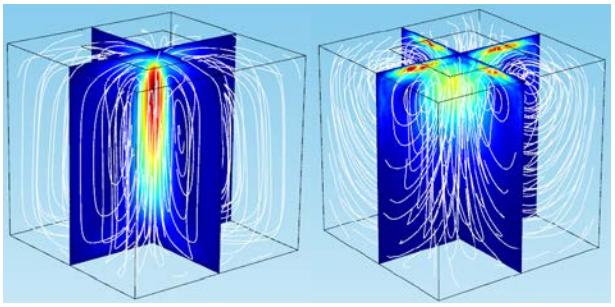

Figure 3 Streamlines and velocity magnitude for (a)ε = 0.8, Ra = 10^3, Da=0.001 (left) and ε = 0.8, Ra = 10^3, Da=0.001 (right).

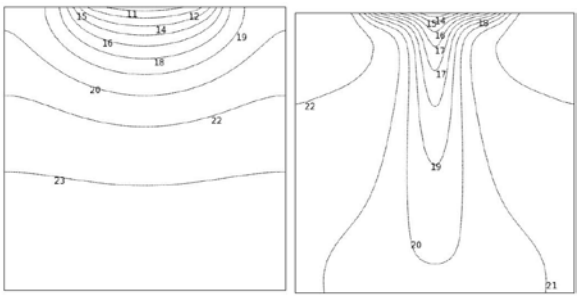

Figure 4. Isothermal contours for ε = 0.8, Da = 10^{-3}, Ra = 10^3 (left) and ε = 0.8, Da = 10^{-3}, Ra = 10^5 (right).

In Figure 4, isothermal contours are plotted at different Rayleigh numbers for fixed porosity and Darcy number. The Rayleigh number gives the ratio of buoyancy forces to change in viscous forces. Higher Rayleigh numbers allow the flow field and thermal gradient to penetrate deeper vertically, elongating the streamlines due to the domination of buoyancy forces. This also results in the decreased diameter and elongation of the toroidal vortex, as the two counter-rotating vortices move vertically and laterally toward the bottom and center of the cube, respectively. At low Rayleigh numbers, the isotherms indicate the predominace of conduction heat transfer,

while convective effects dominate at Ra > 10^4 [18]. However, even at high Rayleigh numbers, conduction is still dominant near the partial top surface boundary condition. This is evident by the close proximity of the isothermal contours, indicating a larger thermal gradient and therefore higher local heat transfer coefficient.

Porosity ε, also known as the void fraction, is the measure of the empty space in a material defined by the ratio of the volume of voids to the total volume. Figure 5 shows the velocity magnitudes looking down the vertical centerline of the cube for ε = 0.4 and ε = 0.8 with constant Rayleigh and Darcy numbers. The results of Figure 5 show that velocity magnitudes are larger with higher porosity. Higher porosity media correspond to higher permeability, which allows greater flow velocity due to smaller boundary and inertial effects [22].

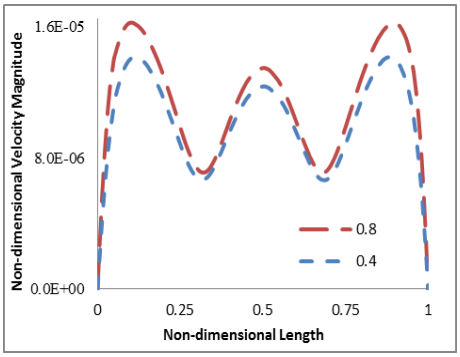

Figure 5. Velocity magnitudes along central vertical axis for various porosities with Da = 10^{-3} and Ra = 10^4

The influence of the Darcy number on isothermal contours is shown in 6. The Darcy number, which is directly proportional to the ratio of permeablility to the square of the length scale, are set to 10^{-3} and 10^{-5} for fixed porosity and Rayleigh number. The smaller Darcy number flow has a lower permeability which generates a force opposing the flow subsequently suppressing the driving thermal plumes. This is evident in the isothermal contours shown in Figure 6 which shows the isothermal contours in three dimensions for the same porosity and Rayleigh numbers shown in Figure 3.

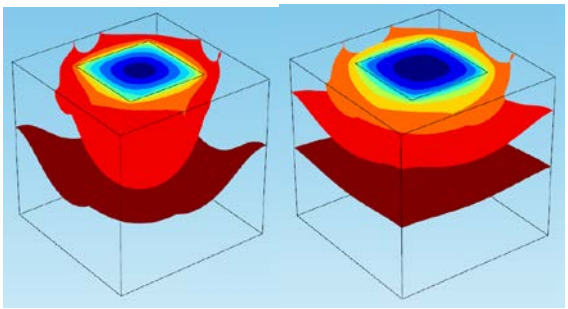

Figure 6. Isothermal contours at y = 0.5 for ε = 0.8, Ra = 10^4Da = 10^{-3} (left) and at y = 0.5 for ε = 0.8, Ra = 10^4,Da = 10^{-5} (right).

The behavior shown in Figure 6 reinforces the smaller Darcy number's flow impedance, highlighed in the lower portion where the temperature differences are very small and viscous effects are strong. As the Darcy number approaches zero, convective heat transfer is significantly reduced while conductive heat transfer dominates. The isothermal contours in Figure 7 illustrate the influence of higher velocities, where porosities ε = 0.4 and ε = 0.8 are overlaid.

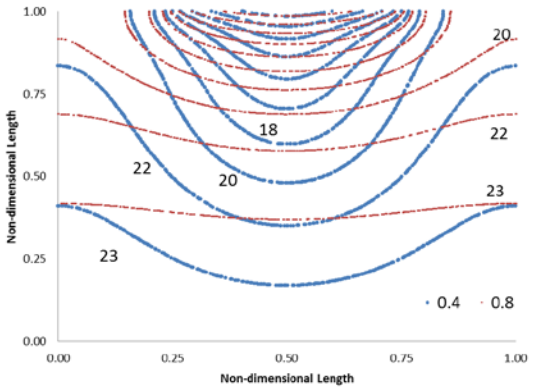

Figure 7. Isothermal contours for Da = 10^{-3}, Ra = 10^4, and ε = 0.4 and ε = 0.8

For comparison purposes, in Figure 7, the values for Darcy and Rayleigh number are identical to those used in Figure 5. The isothermal contours of Figure 7 are more condensed for larger porosity. This agrees with previous studies that as porosity increases the temperature variations become steeper, increasing the heat transfer rate as well as the amount of convective heat transfer [23].

CONCLUSIONS

A parametric study for natural convection inside a fluid-saturated isotropic porous medium with partial top surface convection and internal heat generation has been performed. The Rayleigh number, Darcy number, and porosity were varied to determine their influence on the velocity field and isothermal profiles. The Brinkman-extended Darcy model was implemented and solved using the Galerkin finite element method and validated using a benchmark against previously published work. It was determined that the boundary conditions resulted in the formation of a toroidal vortex due to buoyancy, evident in the three-dimensional streamlines and as two symmetric counter-rotating vortices in the central x and y planes. Higher Rayleigh numbers resulted in elongation of these vortices, allowing the isothermal contours to penetrate deeper into the domain. Larger Darcy numbers lead to higher velocities and more convective mixing as higher permeability allowed the thermal gradient to penetrate the porous medium. Higher porosities were found to increase the thermal gradient due to a larger heat transfer coefficient resulting from increased convection.

REFERENCES

[1] J. Imberger, P.F. Hamblin, Dynamics of lakes, reservoirs, and cooling ponds, A Rev. Fluid Mech 14 (1982) 153-187.

[2] Gabor, J.D., Baker Jr., L, Cassulo, JC, Mansoori, GA. Heat transfer from heat-generating boiling pools. AICHE Symp Series 1978;73:78.

[3] Baker Jr. L, Faw RE, Kulacki FA. Post-Accident heat removal. I. Heat transfer within an internally heated, non-boiling liquid layer. Nucl Sci Eng 1976;61:222

[4] Moraga, N.O., Corvalan, F., Escudey, M., Arias, A., Zambra, C.E., Unsteady 2D coupled heat and mass transfer in porous media with biological and chemical heat generations, International Journal of Heat and Mass Transfer 52 (2009) 5841-5848

[5] L.R. Mealey, J.H. Merkin, Steady finite Rayleigh number convective flows in a porous medium with internal heat generation, International Journal of Thermal Sciences 48 (2009) 1068-1080.

[6] Jawdat, J.M, Hashim, I., Low Prandtl number chaotic convection in porous media with uniform internal heat generation, International Communications in Heat and Mass Transfer 37 (2010) 629-636

[7] Bagai, S., Nishad, C., Free convection in a non-Newtonian fluid along a horizontal plate embedded in porous media with internal heat generation, International Communications in Heat and Mass Transfer 39 (2012) 537-540

[8] Bhadauria, B.S., Kumar, A., Kumar, J., Sacheti, N.C., Chandran, P., Natural convection in a rotating anisotropic porous layer with internal heat generation, Transp Porous Med (2011) 90: 687-705

[9] Reddy, B.V.K., Narasimhan, A., Heat generation effects in natural convection inside a porous annulus, International Communications in Heat and Mass Transfer 37 (2010) 607-610

[10] Saleh, H., Hashim, I., Conjugate Natural Convection in a Porous Enclosure with Non-Uniform Heat Generation, Transp of Porous Med (2012) 94: 759-744

[11] Leal, M.A., Machado, H.A., Cotta, R.M., Integral transform solutions of transient natural convection in enclosures with variable fluid properties, International Journal of Heat and Mass Transfer 43 (2000) 3977-3990

[12] Shivakumara, I.S., Nanjundappa, C.E., Chavaraddi, K.B., Darcy-Benard-Marangoni convection in porous media, International Journal of Heat and Mass Transfer 52 (2009) 2815-2823

[13]Badruddin, I.A., Al-Rashed, A., Ahmed, N.J. S., Kamangar, S., Jeevan, K., Natural convection in a square porous annulus, International Journal of Heat and Mass Transfer 55 (2012) 7175-7187

[14] Char, M.I., Chen, C.C., Effect of a non-uniform temperature gradient on the onset of oscillatory Benard-Marangoni convection of an electrically conducting liquid in a magnetic field, International Journal of Engineering Science 41 (2003) 1711-1727

[15] Vishnampet, R., Narasimhan, A., Babu, V., High Rayleigh Number Natural Convection Inside 2D Porous Enclosures Using the Lattice Boltzmann Method. ASME Journal of Heat Transfer 133 (2011) 062501, 1-9

[16] Kramer, J., Ravnik, J., Jecl, R., Skerget, L., Simulation of 3D flow in porous media by boundary element method, Engineering Analysis with Boundary Elements 35 (2011) 1256-1264

[17] Pakdee, W., Rattanadecho, P., Unsteady effects on natural convection heat transfer through porous media in cavity due to top surface partial convection, Applied Thermal Engineering 26 (2006) 2316-2326

[18] Nithiarasu, P., Seetharamu, K.N., Sundararajan, T., Natural convective heat transfer in a fluid saturated variable porosity medium, International Journal of Heat Mass Transfer 40 (1999) 3955-3967

[19] Brinkman, H.C., On the permeability of media consisting of closely packed porous particles, Appl. Sci. Res. 1 (1947) 81-86

[20] Sengupta, T.K., Talla, S.B., Pradhan, S.C., Galerkin finite element methods for wave problems, Sadhana Vol 30, part 5 (2005) 611-623

[21] Comsol Multiphysics User's Guide, Version 4.2, Comsol

[22] Pakdee, W., Rattanadecho, P., Natural Convection in a Saturated Variable-Porosity Medium Due to Microwave Heating, ASME Journal of Heat Transfer 133 (2011) 062502: 1-8

[23] Beithou, N., Albayrak, K., Abdulmajeed, A., Effects of Porosity on the Free Convection Flow of Non-Newtonian Fluids Along a Vertical Plate Embedded in a Porous Medium, Tr. J. of Engineering and Environmental Science 22 (1998) 203-209